



An Approach to the Health Monitoring of the Fuel System of a Turbofan

Benjamin Lamoureux, Jean-Rémi Massé, Nazih Mechbal

► To cite this version:

Benjamin Lamoureux, Jean-Rémi Massé, Nazih Mechbal. An Approach to the Health Monitoring of the Fuel System of a Turbofan. IEEE Conference on Prognostics and Health Management, 2012, Denver, United States. pp.1-6, 10.1109/ICPHM.2012.6299528 . hal-01100554

HAL Id: hal-01100554

<https://hal.science/hal-01100554>

Submitted on 6 Jan 2015

HAL is a multi-disciplinary open access archive for the deposit and dissemination of scientific research documents, whether they are published or not. The documents may come from teaching and research institutions in France or abroad, or from public or private research centers.

L'archive ouverte pluridisciplinaire **HAL**, est destinée au dépôt et à la diffusion de documents scientifiques de niveau recherche, publiés ou non, émanant des établissements d'enseignement et de recherche français ou étrangers, des laboratoires publics ou privés.



Science Arts & Métiers (SAM)

is an open access repository that collects the work of Arts et Métiers ParisTech researchers and makes it freely available over the web where possible.

This is an author-deposited version published in: <http://sam.ensam.eu>
Handle ID: <http://hdl.handle.net/10985/9175>

To cite this version :

Benjamin LAMOUREUX, Jean-Rémi MASSÉ, Nazih MECHBAL - An Approach to the Health Monitoring of the Fuel System of a Turbofan - In: IEEE Conference on Prognostics and Health Management, United States, 2012 - IEEE PHM 2012 - 2012

Any correspondence concerning this service should be sent to the repository
Administrator : archiveouverte@ensam.eu

An Approach to the Health Monitoring of the Fuel System of a Turbofan

Benjamin Lamoureux, Jean-Rémi Massé
Systems Division Research and Development
SAFRAN Snecma
Villaroche, France
benjamin.lamoureux@sneema.fr

Nazih Mechbal
Laboratory PIMM
Arts et Métiers ParisTech
Paris, France
nazih.mechbal@ensam.eu

Abstract— This paper focuses on the monitoring of the fuel system of a turbofan which is the core organ of an aircraft engine control system. The paper provides a method for real time on-board monitoring and on-ground diagnosis of one of its subsystems: the hydromechanical actuation loop. First, a system analysis is performed to highlight the main degradation modes and potential failures. Then, an approach for a real-time extraction of salient features named indicators is addressed. On-ground diagnosis is performed through a learning algorithm and a classification method. Parameterization of the on-ground part needs a reference healthy state of the indicators and the signatures of the degradations. The healthy distribution of the indicators is measured on field data whereas a physical model of the system is utilized to simulate degradations, quantify indicators sensibility and construct the signatures. Eventually, algorithms are deployed and statistical validation is performed by the computation of key performance indicators (KPI).

Keywords— Health Monitoring, Diagnosis, Hydromechanical Systems, Actuation Loop, Servovalve, Cylinder, Classification

I. INTRODUCTION

In aeronautics, the severity of operational availability requirements combined with the increasing complexity of systems gives interest to prognostics and health management (PHM). Standards for PHM according to IEEE are presented in [1]. For aircraft engine manufacturers, PHM is an opportunity to monitor the state of health of the turbofan, to provide a diagnosis support in maintenance and to limit delays and cancellations.

A good state-of-the-art of the main axes of research in PHM can be found in [2] and some of the methods have already been applied in particular in the field of electronics, for example to monitor the remaining useful lifetime of batteries [3]. In France, some PhD works such as [4] or [5] have addressed the issue of modelling a multi-levels architecture for a complex system's monitoring process or formalizing the prognostics process [6].

In the field of predictive monitoring applied to aeronautics, research is mainly focused on the development of algorithmic methods for diagnosis and prognostics. Some good reviews on

the subject can be found in [7] for the diagnosis and [8] for prognostics.

However, academic research is often detached from the industrial needs on the following points: (1) health monitoring is currently restricted to captor faults, vibration analysis and structural surveillance but health assessment of control systems is rarely addressed; (2) papers commonly make the hypothesis that every variable is measured so indicators are easily constructible but actually, the position and the number of sensors are defined and cannot be changed; (3) the extraction of indicators must be performed on-board and the issues related to the real time in-situ computation is almost never addressed and (4) physical models are necessary to quantify the impacts of degradation and their probable evolution.

This paper is part of a larger project which aims at providing an integrated method for developing a PHM system with emphasis on the indicators construction adapted to in-flight computation requirements and the use of physical models to simulate the degradation impacts. The targeted system for the application is the fuel system of a turbofan, the main organ of the engine control system. This paper focuses on the diagnosis of the following subsystem: an actuation loop dedicated to the position control of a variable geometry. The study will be articulated around five points: System Analysis, Indicators, Degradations Modelling, Indicator Transformation Laws Computation and Statistical Validation of Performances.

II. SYSTEM ANALYSIS

In order to monitor a system, the first step is to determine its degradation modes and it can be achieved through expertise, experience feedback or FMEMA. This study will focus on the mechanical degradations of the system and electrical ones will not be treated.

The system is a closed loop composed of three main components: A controller, a servovalve and a cylinder. The position of the cylinder is measured by a linear variable differential transformer (LVDT), as shown in Fig. 1.

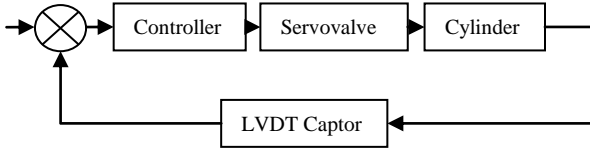


Fig. 1: Schematic of the hydromechanical actuation loop

A.

In this application, the studied servovalve type is two-stage flapper-nozzle. In this type of servovalve, the power transmission chain is the following one:

1. A control current is send to a torque motor
2. The current is converted to a displacement of the flapper through an electromagnetic effect
3. The displacement of the flapper changes the position of the second stage spool via a hydraulic control
4. The position of the spool changes the distribution of the flows. A flapper-nozzle servovalve configuration is shown in Fig. 2.

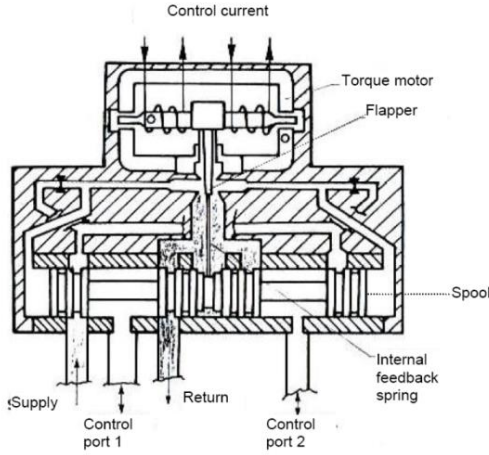


Fig. 2: Electrohydraulic flapper-nozzle servovalve configuration

The following list of the degradation modes selected for the servovalve is inspired by [9]:

- 1) *Increased contamination of the filters:* As dust and debris accumulate in the servovalve, filters gradually lose their efficiency and the hydraulic resistance increases. The result is a slower response of the servovalve.
- 2) *Drift of the null bias current:* As the torque motor ages and loses his magnetic properties, the null bias current of the servovalve, namely the current for which the flows are equal in control ports 1 and 2, can drift from its nominal value.
- 3) *Increased backlash:* With the progressive wear of the internal feedback spring, the hysteresis of the servovalve increases.
- 4) *Increase of the friction force between spool and sleeve:* This phenomenon is due to the cumulative effects of continuous movement of the spool and contamination of the hydraulic fluid because the debris induces a silting effect.

5) *Increase in the radial clearance between spool and sleeve:* Because of the contamination, abrasion of the corners of the spool lands resulting in an increase of internal leakage.

B. Degradation modes of a cylinder

The cylinder considered in this application is a double-acting hydraulic cylinder with a cooling diaphragm between the two sides. The hydraulic fluid used is fuel.

The following list of the degradation modes selected for the hydraulic cylinder is inspired by [10]:

- 1) *Internal leakage between the two sides:* As the seal ages, dust and debris accumulate between the seal and the sleeve resulting in an abrasive effect degrading the cylinder body.
- 2) *Clogging of the cooling diaphragm:* With the increase of the temperature, a coking of the fuel can occur, resulting in the clogging of the diaphragm.

C. Other potential degradation modes

The list of degradation modes presented above is not exhaustive and many other phenomenons can occur such as a damage of the kinematic chain downstream of the cylinder or the burst of a pipe but the choice was made to focus only on the servovalve and cylinder's degradations.

III. INDICATORS

A. Flow Gain curve of a Servovalve

Among the different measures characterizing a servovalve, the flow gain curve is one of the most significative because it displays both static and dynamic features as shown in Fig. 3.

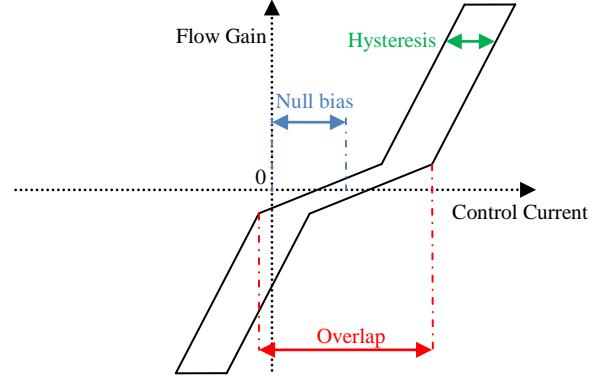


Fig. 3: Flow Gain curve and main features

The extraction of this curve requires that the servovalve is equipped with flowmeters but in our application, only the position of the cylinder is measured. However, the cylinder's velocity v_{cyl} and the servovalve output flows in each control port Q_{SV_head} and Q_{SV_rod} can be linked via the simplified equation:

$$v_{cyl} = \begin{cases} (Q_{SV_head} - Q_{cooling}) / S_{head} & \text{during shaft outlet} \\ -(Q_{SV_rod} - Q_{cooling}) / S_{rod} & \text{during shaft inlet} \end{cases} \quad (1)$$

Where $Q_{cooling}$ is the cooling flow between the two sides of the cylinder and S_{head} and S_{rod} are respectively the cross-sectional area of the head and the rod sides.

B. Velocity Gain of a hydromechanical loop

In order to get around the lack of flowmeters to monitor the servovalve only, the idea is to monitor the whole loop by following salient features on the Velocity Gain curve.

This curve can be obtained only with the measures of both the control current $I_{control}$ and the cylinder's velocity V_{cyl} . The value of V_{cyl} is computed by derivation of the cylinder's position X_{cyl} .

Blue points in Fig. 4 are the result of an extraction of the velocity gain curve performed during an entire flight. Because of the hysteresis of the servovalve, the dispersion of the points is substantial and therefore a smoothing algorithm based on local means is applied to the data.

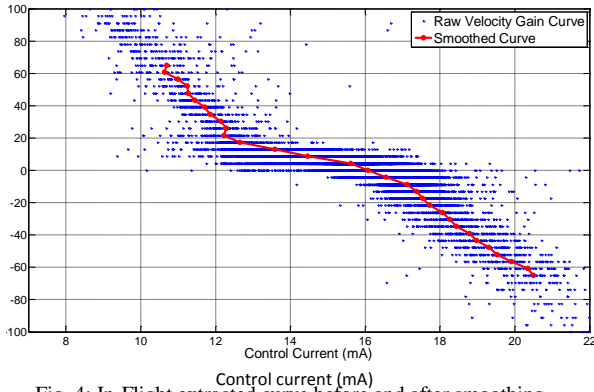


Fig. 4: In-Flight extracted curve before and after smoothing

C. Indicators Construction

From the extracted curve, we define many indicators related to the targeted degradation. Those indicators are listed in Table I and their graphical equivalent is shown in Fig. 5.

TABLE I
INDICATORS EXTRACTED FROM THE CURVE

Names		Targeted degradations
Long	Short	
Slope change #1 abscissa	X_1	Degradations impacting the horizontal position of the curve → Increase of the radial clearance between spool and sleeve
Slope change #1 ordinate	Y_1	Degradations impacting the vertical position of the curve → Diaphragm clogging, cylinder internal leakage
Slope change #2 abscissa	X_2	Idem X_1
Slope change #2 ordinate	Y_2	Idem Y_1
Null Bias Current $I_{nb} = \frac{X_1 + X_2}{2}$	I_{nb}	Degradations impacting the value of the Null Bias → Null Bias current shift
Idle Current of the Loop (Current for null velocity)	I_0	Degradations impacting the static behaviour of the loop → All the degradations

Standard Deviation (hysteresis) at idle current	Hys_0	Degradations impacting the hysteresis → Increased Backlash
Velocity Gain for Shaft Inlet	G_{in}	Degradations impacting the global dynamic behaviour of the loop → Increased Backlash, Contamination of the filters, Increased friction force
Velocity Gain for Shaft Outlet	G_{out}	Idem G_{in}
Velocity Gain for Null Region	G_{null}	Idem G_{in}

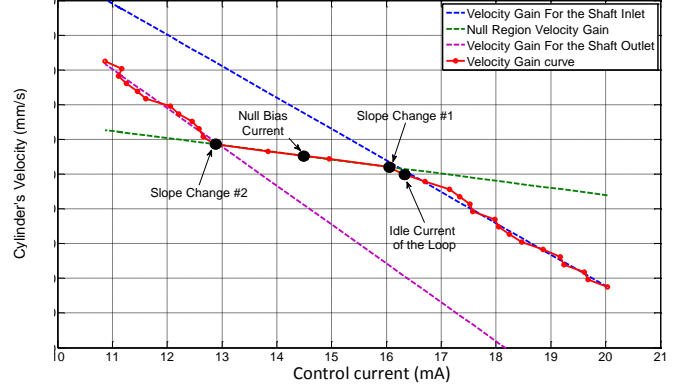


Fig. 5: Graphical representation of the indicators

IV. DEGRADATIONS MODELLING

A. Model and Sub-models Construction

A physical model of the hydromechanical system has been developed in Matlab-Simulink® in order to simulate its behaviour in presence of some degradation and to quantify their impacts. This model is composed of three sub-models: Servovalve, cylinder and controller. The granularity of the sub-models must be important enough to simulate all the degradations discussed in the system analysis. For example, the sub-model of the servovalve, the most complex one, must include the modelling of the two-stages, the filters and the feedback spring. A good method for modelling servovalves is given in [11].

There are two ways degradations can be modelled: additive and multiplicative. The former consists in adding a value to some parameters and the latter consists in a multiplication of some parameters as shown in Fig. 6. In Fig. 6, Y_u and U are healthy values of variables, f is the degradation intensity and Y is the degraded value of variables.

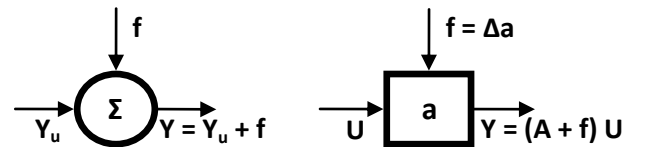


Fig. 6: Additive and Multiplicative modelling of degradations

TABLE III
MODELLING OF DEGRADATIONS

Degradation	Modelling
Increased contamination of the filters	<i>Multiplicative:</i> To simulate a decrease of the efficiency, the flow is multiplied by a scalar in the range [0,1]
Drift of the null bias current	<i>Additive:</i> A value corresponding to the opposite of the drift is added to the control current.
Increased Backlash	<i>Multiplicative:</i> Modification of the transfer function governing the position of the spool in the second stage.
Increase of the friction force	<i>Additive:</i> Increase of the coefficient of friction between spool and sleeve.
Increase in the radial clearance	<i>Additive:</i> Decrease of the restriction coefficient at the corners of the spool lands victims of abrasion.
Internal leakage between the two sides	<i>Additive:</i> Increase of the restriction coefficient of the cooling flow
Clogging of the cooling diaphragm	<i>Additive:</i> Decrease of the restriction coefficient of the cooling flow

B. Recalibration of the model

The main hypothesis of this method is that operational data are available. Thus, it is supposed that the distribution of the indicators corresponding to a healthy state is well known.

For each simulation, the goal is to compute the velocity gain of the system by simulating the velocity of the cylinder for a gradually increasing control current from lower saturation boundary to upper saturation boundary.

Before simulating the degraded states, it is necessary to simulate and recalibrate the model parameters against operational data for the reference healthy state. Fig. 7 shows both extracted and estimated velocity gain curves for the healthy state. The estimated one is obtained from a model configured with averaged parameters given by constructors. The result after recalibration on parameters is also given in Fig. 7, and it can be noted that a difference remains between the curves around the idle current of the loop. The model used in this application is not enough accurate to explain this local deviation.

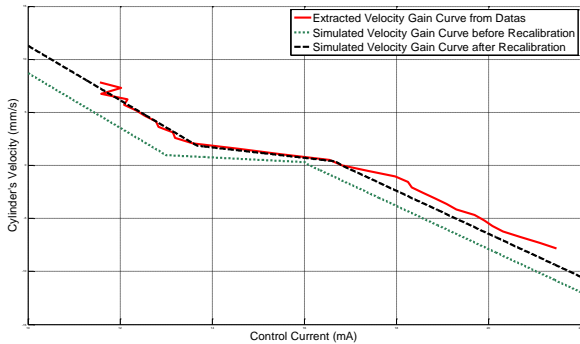


Fig. 7: Extracted against Estimated Velocity Gain of the healthy state

C. Simulation of the degradations

For this paper, the focus will be on only two degradations namely the drift of the null bias current of the servovalve and the internal leakage between the two sides of the cylinder.

Results of the simulation on the recalibrated model with those two degradations are given in Fig. 8.

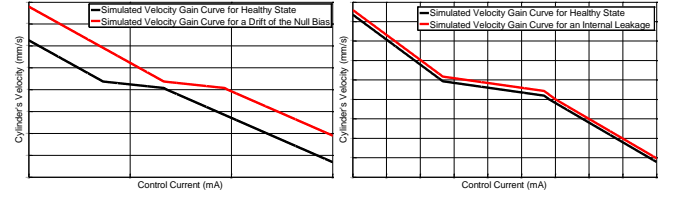


Fig. 8: (a) Left: effect of a null bias drift. (b) Right: effect of an internal leakage in the cylinder

V. INDICATORS TRANSFORMATION LAW COMPUTATION

A. Construction of the laws

In this part, a design of experiment is generated to organize the simulations of the behaviour of the system in presence of degradations. For each case, simulations are run for gradually increasing intensities of degradation. Eventually, the results are summarized in the form of indicators transformation laws (ITL).

With Ind_i representing the i^{th} indicator in a healthy state, Ind_i^{deg} the i^{th} indicator in presence of the degradation deg , and Int^{deg} the intensity of the degradation deg , the ITL named F_i^{deg} corresponding to the i^{th} indicator and the degradation deg can be defined as follows:

$$Int^{deg} \xrightarrow{F_i^{deg}} \Delta I_i^{deg} = A_i^{deg} Int^{deg} \quad (2)$$

where A_i^{deg} is the coefficient of the linear regression of ΔI_i^{deg} with respect to Int^{deg} . ΔI_i^{deg} is the change in the value of the indicator and can be also expressed this way:

$$\Delta I_i^{deg} = Ind_i^{deg} - Ind_i \quad (3)$$

Thus, F_i^{deg} provides the change in the indicator's value for a given intensity of degradation.

B. Utilization of the laws

Once computed, an ITL makes it possible to generate an estimated value of indicators for a degraded state from a healthy value computed from operational data according to the following equation:

$$I_i^{deg} = I_i^{healthy} + \Delta I_i^{deg} \quad (4)$$

In this application, 7 degradations and 10 indicators are considered, which means that 70 ITL must be computed. For instance, the law giving the value of X_1 for the degradation drift of the null bias current is:

$$I_{X_1}^{NB\ drift} = I_{X_1}^{healthy} + A_{X_1}^{NB\ drift} Int^{NB\ drift} \quad (5)$$

Where $I_{X_1}^{healthy}$ is computed by averaging the extracted value of X_1 for a given number of flights for which the system is considered flawless.

VI. STATISTICAL VALIDATION OF PERFORMANCES

A. Key Performance Indicators

For this application, both fault detection and diagnosis are addressed. A presentation and definition of Key Performance Indicators (KPI) is given in Table III.

TABLE III
KEY PERFORMANCE INDICATORS

KPI	Definition
False Positive Rate	Proportion of False Positive (false alarm) among all the states where a fault is detected (see Fig. 9)
False Negative Rate	Proportion of False Negative (undetected faults) among all the states where no fault is detected (see Fig. 9)
False Classification Rate	Proportion of False Classification among all classifications
Robustness	Capacity of the monitoring system to be still efficient when some parameters drift from their nominal values.

		Estimated Condition	
		No Fault	Fault
Actual Condition	No Fault	NFD	FP
	Fault	FN	FD

Fig. 9 : Condition Assessment Matrix

B. Method for fault detection and diagnosis

A more precise presentation of the method presented below can be found in [12].

1) Indicators Model Learning:

The first step is to learn a Gaussian model of the indicators distribution in a reference state, typically a healthy state. The model is learned from extracted indicators on a given number of flights and is presented as follows:

$$Model(i) = \begin{pmatrix} \mu_i^{healthy} \\ \sigma_i^{healthy} \end{pmatrix} \quad (6)$$

where $\mu_i^{healthy}$ is the mean of the indicators and $\sigma_i^{healthy}$ their standard deviation.

2) Fault Detection:

It is based on an abnormality score named Z_{score} . For the indicator i , $Z_{score,i}$ is defined as follows:

$$Z_{score,i} = \frac{I_i - \mu_i^{healthy}}{\sigma_i^{healthy}} \quad (7)$$

where I_i is the currently measured value of indicator.

Then a global abnormality score of the system $Global_Z_{score}$ is computed from $Z_{score,i}$ with $i \in [1; 10]$ via the Mahalanobis distance [13].

Indicators are extracted on-board and $Global_Z_{score}$ is computed on-ground at each flight. The parameterization of the fault detection consists in defining a relevant threshold value Thr and if the value of $Global_Z_{score}$ crosses Thr , it means that a fault has been detected.

3) Diagnosis:

Diagnosis is performed via a classification of signatures. A signature is a vector of indicators. For this application, a signature is a vector appending 10 indicators extracted from flight data:

$$Sign = (Z_{score,X_1}, Z_{score,Y_1}, \dots, Z_{score,G_{null}})^T \quad (8)$$

If the system is healthy, $Sign$ is a zero vector of size 10.

Assuming that the maximal intensities of the degradations are known, it is possible to determine the signatures of the degradations $Sign_{ref,deg}$ associated.

$$Sign_{ref,deg} = \left(\frac{I_{X_1}^{deg} - \mu_{X_1}^{healthy}}{\sigma_{X_1}^{healthy}}, \dots, \frac{I_{G_{null}}^{deg} - \mu_{G_{null}}^{healthy}}{\sigma_{G_{null}}^{healthy}} \right)^T \quad (9)$$

When a fault is detected, the classification algorithm is run. This algorithm is based on a pattern recognition method which finds the reference signature that most closely matches the currently measured signature. A guilt probability is assigned to each component of the system.

C. Statistical Validation

1) Matrix of the signatures

To perform fault detection and diagnosis, it is essential to determine the matrix of the signatures. It shows the signature corresponding to the maximal intensity of the degradations. A part of this matrix, taking into account only two degradations is given in Table IV.

TABLE IV
MATRIX OF THE SIGNATURES

Degradation	Influences (Z_{scores})									
	X_1	Y_1	X_2	Y_2	I_{nb}	I_0	Hys_0	G_{in}	G_{out}	G_{null}
Drift of the null bias current	24	0	26	0	28	24	0	0	0	0
Internal leakage between the two sides	0	4	0	11	0	1	0	0	0	0

2) Performances of fault detection

Once the matrix of the signatures is available, a detection threshold Thr on the global score $Global_Z_{score}$ must be defined.

The value of this threshold must be low enough to ensure detection of all the different degradation, even those not

provided by the system analysis and high enough to ensure a low rate of false alarms. To set this value in an optimal way, it is essential to take into account the standard deviation of the $Global_Z_{score}$.

First, the computation of the maximum likelihood function of $Global_Z_{score-healthy}$ is performed to set a first value of Thr , as shown in Fig. 10. In this paper, the likelihood function is a Gaussian and its parameters are the mean $\mu_{healthy}$ and the standard deviation $\sigma_{healthy}$. Typically, the chosen value for Thr is:

$$Thr = \mu_{healthy} + A \cdot \sigma_{healthy} \quad (10)$$

At first approach, the chosen value for A is $A = 2$ because it ensures only 5% of false detection. However, this value can potentially limit the false negative rate, so it is necessary to check if the degradations are still detectable.

To ensure the performances, the distributions of $Global_Z_{score-healthy}$, $Global_Z_{score-leak}$ and $Global_Z_{score-drift}$ are compared as presented in Fig. 10.

Performances for different values of A are proposed in Table V.

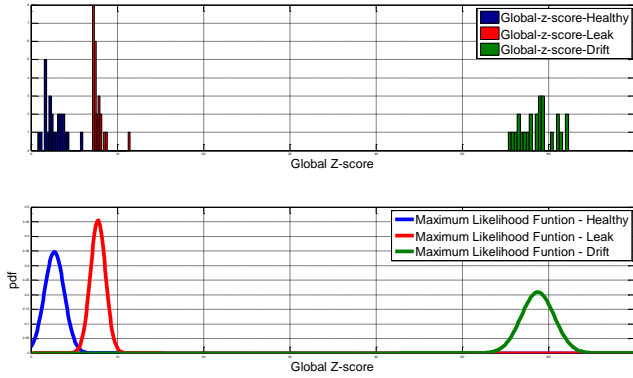


Fig. 10 : Distribution of Global_scores and likelihood functions

TABLE V
FAULT DETECTION PERFORMANCES

A	Null Bias Drift		Internal Leakage	
	False Positive Rate	False Negative Rate	False Positive Rate	False Negative Rate
0	0%	0%	50%	0%
1	0%	0%	16%	0%
2	0%	0%	3%	0%
3	0%	0%	0.3%	2%
5	0%	0%	0%	6%

3) Performances of diagnosis

The classification algorithm gives, for each component of the system, a probability of guilt proportional to the collinearity between the current signature and the referenced signatures. The diagnosis performances depend on the intensity of the degradations. Results are shown in Table VI.

TABLE VI
DIAGNOSIS PERFORMANCES

Effective Degradation	Percentage of max intensity (From ITL)	Probability of guilt of Drift	Probability of guilt of Leak
Drift	25%	0.94	0.06
Drift	50%	0.94	0.06
Drift	100%	0.94	0.06
Leak	25%	0.37	0.63
Leak	50%	0.13	0.87
Leak	100%	0.11	0.89

VII. CONCLUSIONS

This paper provides a methodology to perform fault detection and diagnosis on a hydromechanical actuation loop. A first part details how to construct relevant indicators to perform on-board extraction of indicators and a second part how to achieve and validate fault detection and diagnosis on-ground. It must be noted that further works will follow, dealing with the management of uncertainties, the architecture of monitoring for a wider system and also prognostics.

REFERENCES

- [1] J. W. Sheppard, M. A. Kaufman, and T. J. Wilmer, "IEEE Standards for Prognostics and Health Management," *Aerospace and Electronic Systems Magazine*, vol. 24, no. 9, p. 34–41, 2009.
- [2] A. Jardine, D. Lin, and D. Banjevic, "A review on machinery diagnostics and prognostics implementing condition-based maintenance," *Mechanical systems and signal processing*, vol. 20, no. 7, p. 1483–1510, 2006.
- [3] B. Saha and K. Goebel, "Uncertainty management for diagnostics and prognostics of batteries using Bayesian techniques," in *IEEE Aerospace Conference*, Big Sky, 2008, p. 1–8.
- [4] A. Muller, *Contribution à la maintenance prévisionnelle des systèmes de production par la formalisation d'un processus de pronostic*. PhD thesis from the Nancy I University - Henri Poincaré, 2005.
- [5] P. Ribot, *Vers l'intégration diagnostic-pronostic pour la maintenance des systèmes complexes*. PhD thesis from the Toulouse III University - Paul Sabatier, 2009.
- [6] P. Cochetoux, *Contribution à la maintenance proactive par la formalisation du processus de pronostic des performances de systèmes industriels*. PhD thesis from the Nancy I University - Henri Poincaré, 2010.
- [7] A. Patterson-Hine, G. Biswas, S. Aaseng, S. Narasimhan, and K. Pattipati, "A Review of Diagnostic Techniques for ISHM Applications," vol. 1st Integrated Systems Health Engineering and Management Forum, 2005.
- [8] M. Roemer, C. S. Byington, G. Kacprzynski, and G. Vachtsevanos, "An overview of selected prognostic technologies with application to engine health management," in *Proceedings of GT2006 ASME Turbo Expo*, Barcelona, 2006.
- [9] L. Borello, M. D. Vedova, G. Jacazio, and M. Sorli, "A Prognostic Model for Electrohydraulic Servovalves," *Annual Conference of the Prognostics and Health Management Society*, 2009.
- [10] P.-Y. Crepin and R. Kress, "Model Based Fault Detection for an Aircraft Actuator," in *22nd Congress of International Council of the Aeronautical Sciences*, Harrogate, 2000.
- [11] B. Attar, *Modélisation réaliste en conditions extrêmes des servovalves électrohydrauliques utilisées pour le guidage et la navigation aéronautique et spatiale*. Thèse de l'Université de Toulouse, délivré par l'INSA de Toulouse, 2008.
- [12] J. Lacaille, "Standardized failure signature for a turbofan engine," in *Aerospace conference, 2009 IEEE*, Big Sky, MT, 2009, pp. 1–8.
- [13] R. De Maesschalck, D. Jouan-Rimbaud, and D. Massart, "The mahalanobis distance," *Chemometrics and Intelligent Laboratory Systems*, vol. 50, no. 1, pp. 1–18, 2000.